Journal of Power Sources 224 (2013) 152–157

Contents lists available at SciVerse ScienceDirect

Journal of Power Sources

journal homepage: www.elsevier.com/locate/jpowsour

Single-step in-situ preparation of thin film electrolyte for quasi-solid state quantum dot-sensitized solar cells

Shen Wang [a,b,c], Quan-Xin Zhang [a,b,c], Yu-Zhuan Xu [a,b,c], Dong-Mei Li [a,b,c], Yan-Hong Luo [a,b,c], Qing-Bo Meng [a,b,c,*]

[a] Key Laboratory for Renewable Energy, Chinese Academy of Sciences, Beijing 100190, China
[b] Beijing Key Laboratory for New Energy Materials and Devices, Beijing National Laboratory for Condense Matter Physics, Beijing 100190, China
[c] Institute of Physics, Chinese Academy of Sciences, Beijing 100190, China

HIGHLIGHTS

- In-situ preparation for the thin film electrolyte and Cu_2S electrode in one step.
- As high conversion efficiency as the liquid-based QDSCs.
- Good stability of polysaccharide-based quasi-solid state QDSCs.

GRAPHICAL ABSTRACT

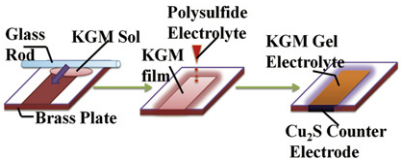

ARTICLE INFO

Article history:
Received 21 May 2012
Received in revised form
27 August 2012
Accepted 14 September 2012
Available online 2 October 2012

Keywords:
Quantum dot-sensitized solar cells
Polysaccharide
Konjac glucomannan
Quasi-solid state electrolyte
Ionic conductivity

ABSTRACT

Natural polysaccharide Konjac glucomannan (KGM) is, for the first time, applied as the polymer matrix for thin film gel electrolyte in CdS/CdSe quantum dot-sensitized solar cells (QDSCs). The predominance of this thin film quasi-solid state QDSCs lies in the in-situ preparation of the electrolyte and Cu_2S counter electrode in one step without mold, which can significantly simplify the cell fabrication process. The cell based on this electrolyte presents an energy conversion efficiency of 4.0% under AM 1.5 illumination of 100 mW cm^{-2} with excellent stability compared to that of liquid-based QDSCs.

1. Introduction

Since 1991, increasing attention has been paid on dye-sensitized solar cells (DSCs) due to their relatively high efficiency, low cost and easy fabrication [1,2]. Apart from the organic or organometallic dyes, inorganic semiconductor quantum dots (QDs), such as CdS, CdSe, PbS, InP and PbSe, have also been a kind of promising sensitizers for DSCs, which are known as quantum dot-sensitized solar cells (QDSCs) [3]. Some attractive advantages including the tunable band gaps, high molar extinction coefficient and facile preparation of QDs have brought QDSCs a bright future in the photovoltaic field. Especially, the efficiency of QDSCs might be further improved to 44% with the utilization of hot electrons [4] and multiple exciton generation [5]. Recently, around 5% of efficiency of CdS/CdSe QDSCs has already been achieved [6–9].

At present, aqueous polysulfide electrolyte is commonly used in QDSCs because most of the QDs are not stable in the conventional I^-/I_3^- electrolyte. For example, to the CdSe-based QDSCs, a $CdSe_{1-x}S_x$ layer could be spontaneously formed at the electrolyte/QDs interface, which might be helpful to prevent further corrosion [10]. However, the aqueous polysulfide electrolyte is easy to leak and evaporate, which is disadvantageous to the long-term stability of QDSCs.

* Corresponding author. Key Laboratory for Renewable Energy, Chinese Academy of Sciences, Beijing 100190, China. Tel./fax: +86 10 82649242.
E-mail address: qbmeng@iphy.ac.cn (Q.-B. Meng).

0378-7753/$ – see front matter © 2012 Elsevier B.V. All rights reserved.
http://dx.doi.org/10.1016/j.jpowsour.2012.09.044

Quasi-solid state polymer gel electrolyte shows high ionic conductivity, well thermal stability and favorable penetration ability into the nanocrystalline porous TiO_2 films, thus it has been widely used in DSCs. In general, the polymer gelator in the electrolyte has a cross-linking network, in which the liquid electrolyte is trapped to form homogeneous quasi-solid state electrolyte. The strong affinity between the gelator and the liquid electrolyte can well restrain the solvent's leakage and evaporation. At the same time, the conductivity of the gel electrolyte is still comparable to that of liquid electrolyte. As a result, high efficiency and good stability of gel electrolyte-based DSCs have been achieved [11–22]. Recently, up to 9.46% of the efficiency has been achieved for gel electrolyte-based DSCs even better than the corresponding liquid electrolyte-based DSCs, indicating a promising application in the future [23]. For the QDSCs, however, there was only one work reported on the quasi-solid state electrolyte which exhibited a promising 4.0% conversion efficiency [24]. However, comparing to the liquid electrolyte-based QDSCs, no further investigation in promoting the stability of QDSCs was presented. Besides, the hydrogel still needs mold to form thin film-like shape.

Biodegradable polysaccharides agarose and carrageenan have been applied as a matrix of quasi-solid state electrolyte in DSCs, showing good cell performance [25–29]. Herein, polysaccharide Konjac glucomannan (KGM) as the polymer matrix has been applied to prepare the quasi-solid state electrolyte in CdS/CdSe QDSCs for the first time [30]. This kind of KGM gel can easily form thin films without using additional mold. To keep the integrality of thin films and simplify the fabrication process of the device, we developed an in-situ preparation method to combine the preparation of both the electrolyte film and counter electrode in one step. By using this method, QDSC can present a conversion efficiency of over 4% under AM 1.5 illumination of 100 mW cm^{-2}, and exhibit good stability after sealing as well.

2. Experimental

2.1. Single-step in-situ preparation of KGM-based hydrogel electrolyte and counter electrode

Konjac glucomannan (purity 98%) was purchased from Bomei Biotechnology in China. 0.5 g KGM powder was dissolved in 100 mL deionized water, stirred at 80 °C for 1 h, then filtered to remove the impurities, and finally evaporated to give the KGM concentration doubled. The single-step in-situ preparation method of KGM gel electrolyte on Cu_2S counter electrode is shown in Fig. 1. The KGM sol was doctor-bladed on HCl-treated brass plate and then heated at 80 °C to remove the water, the thickness of the film was controlled to 25 μm comparable to the spacer in liquid-based QDSCs. After the film was cooled down, the polysulfide electrolyte (1 M Na_2S and 1 M S in water) was added drop-wise onto the film. After removing the surface liquid, both hydrogel electrolyte and counter electrode were formed. The preparation of Cu_2S counter electrode on brass plate was referred to the reference [31].

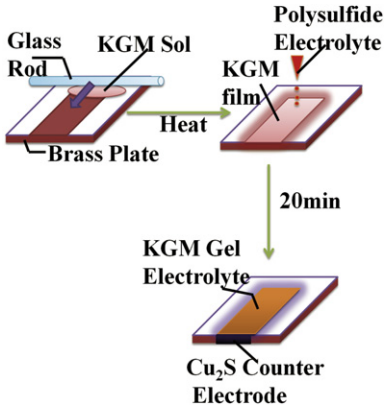

Fig. 1. Single-step in-situ preparation of KGM hydrogel electrolyte and Cu_2S counter electrode.

2.2. Fabrication of the CdS/CdSe co-sensitized solar cells

TiO_2 photoanode was prepared on FTO glass (fluorine-doped tin oxide conducting glass, Pilkington, sheet resistance: 15 Ω square^{-1}, thickness 2.2 mm) by doctor-blading technique [32]. The CdS/CdSe quantum dots were deposited on TiO_2 photoanode by the chemical bath deposition (CBD) technique according to the literature [31]. The deposition durations for CdS and CdSe quantum dots on TiO_2 photoanode were 50 min and 5.5 h, respectively. The temperature of the chemical bath was 10 °C. The photoanode was then passivated with ZnS. The in-situ prepared electrolyte/counter electrode and photoanode were assembled together directly to form the gel electrolyte-based QDSCs (G-QDSCs). As a reference, liquid electrolyte-based QDSCs (L-QDSCs) with the same CdS/CdSe co-sensitized photoanode were fabricated, using liquid polysulfide electrolyte and Cu_2S counter electrode on a brass plate [33]. Silicone spacers (thickness 25 μm) were applied to separate photoanode and counter electrode in L-QDSCs. Spacer-free L-QDSCs were also fabricated for comparison.

2.3. Characterization

The cells were tested under AM 1.5 illumination by Oriel solar simulator 91192 with light intensity of 100 mW cm^{-2}, which was determined by Oriel 70260 radiant power/energy meter. The *J–V* curves were measured based on Princeton Applied Research, Model 263A. A mask with a window of 0.15 cm^2 was fixed on each cell by two clippers to ensure the same test active area. The incident photon to current conversion efficiencies (IPCE) of L-QDSCs and G-QDSCs were measured by DC method using our home-made IPCE instrument [34]. Electrochemical Impedance Spectroscopy (EIS) was measured in dark by using IM6ex Electrochemical Workstation (ZAHNER) under forward bias of 0.6 V. The frequency range was 1×10^5–1×10^{-1} Hz with 10 mV ac amplitude. The ionic conductivities of electrolytes were measured in a 'stainless steel/electrolyte/stainless steel' cell by using ac impedance technique. The frequency range was 2×10^5–5×10 Hz with 10 mV ac amplitude. The EIS data were fitted by Z-view. The morphology of the KGM gel was observed by scanning electron microscope (FEI, S-FEG, XL30) after lyophilizating.

2.4. Stability test

To test the stability of G-QDSCs and L-QDSCs, the cells were sealed as shown in Fig. 2, mainly according to the reference [35]. The Cu_2S counter electrode on brass foil (thickness: 30 μm) and an

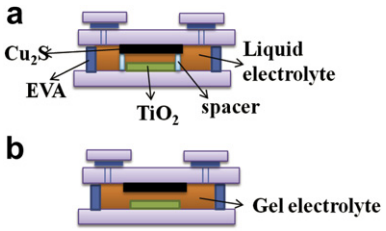

Fig. 2. Structures of sealed QDSCs: (a) L-QDSCs (b) G-QDSCs.

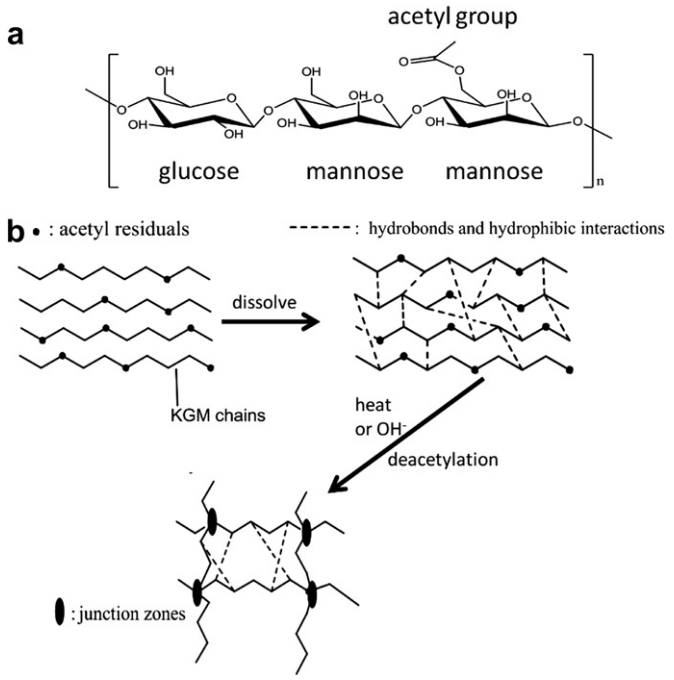

Fig. 3. (a) Structure of KGM. (b) Gelation mechanism of KGM.

EVA (ethylene-vinyl acetate copolymer) film as the sealer were used in sealed QDSCs. Silicone spacers were placed on the counter electrodes to separate TiO_2 and Cu_2S in L-QDSCs. In the sealed G-QDSCs, the preparation of hydrogel electrolyte and counter electrode was also referred to single-step in-situ method.

3. Results and discussion

3.1. Properties of KGM-based hydrogel

KGM which is derived from tubers of *Amorphophallus konjac* is easy to form thermally irreversible gel by heating or under alkaline environment [36]. Its chemical structure is composed of D-mannose and D-glucose monomers, connected by β-1,4-glycosidic bond (Fig. 3(a)). The ratio of mannose/glucose in KGM is nearly 1.6:1; some mannose monomers in polymer chains are acetylated. The gelation mechanism is shown in Fig. 3(b). When dissolved in water, KGM will form thermally reversible hydrogel first through the hydrogen bonding and the hydrophobic effect. By heating or under alkaline environment, deacetylation happens to form a thermally irreversible polymer network [37].

Fig. 4(a) and (b) show the photographs of KGM thin films before and after adsorbing polysulfide electrolyte, respectively. Unlike our previous work [24], KGM can form thin films spontaneously by removing water from the sol. After adsorbing liquid electrolyte, the thin film structure can still be maintained. By measuring the weight of KGM electrolyte, 90 wt% of liquid electrolyte was maintained into the KGM polymer network. This high water-retaining property implies that the electrolyte has a comparable ionic mobility to the liquid electrolyte.

To further understand the structure of KGM thin films, the morphology of KGM is shown in Fig. 4(c). The sample was lyophilized to dryness in order to maintain the structure of KGM. We can see from Fig. 4(c) that the KGM polymer exhibits continuous porous structure. The liquid electrolytes can be well trapped in these pores due to a large number of hydrophilic groups in KGM.

3.2. Merits of single-step in-situ preparation method

For DSCs, the gel electrolyte and counter electrode are usually prepared separately in traditional method [24]. That is, the thin film-like electrolyte in DSCs was prepared on the substrate in advance. After absorbing liquid electrolytes, the film was peeled off from the substrate and then clamped between electrodes. However, there are some disadvantages in this process: The strong affinity between the thin film and the substrate makes it difficult to transfer the whole film. Moreover, the processes in preparing counter electrode and the electrolyte separately are time consuming.

The single-step in-situ preparation method, as shown in Fig. 1, can solve these problems. By using doctor-bladed method, the KGM

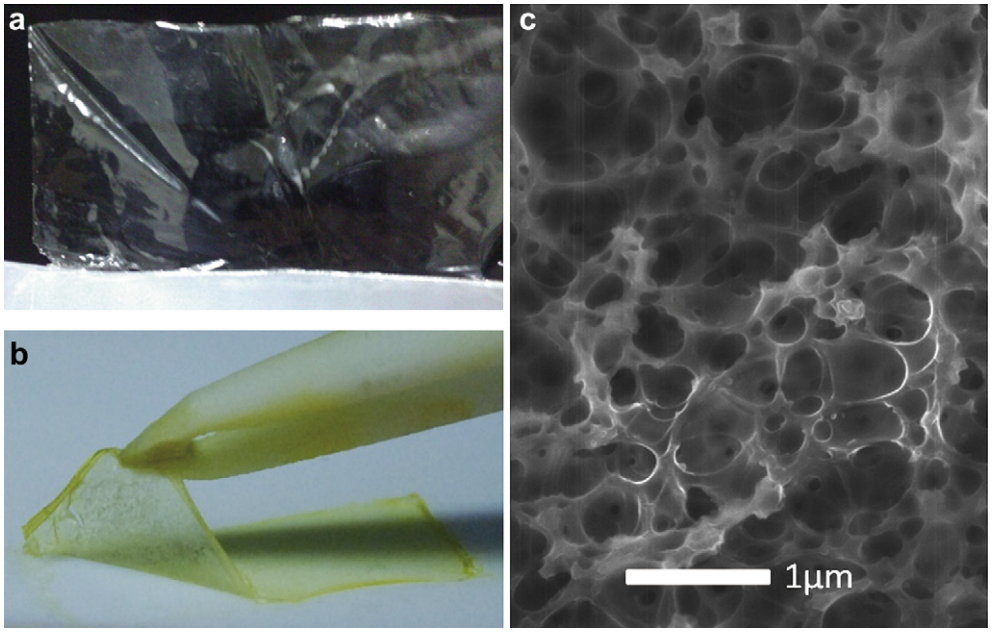

Fig. 4. (a) KGM thin film. (b) KGM thin film after adsorb electrolyte on substrate bended by tweezer. (c) SEM image of KGM thin film.

sol is directly spread on the brass plate. After heating, thermally irreversible polymerization occurs to form the KGM film on the brass plate. When the brass plate is cooled down to room temperature, the polysulfide electrolyte is dropped onto the polymer matrix. After 20 min, the preparation of counter electrode and the adsorption of liquid electrolyte in the KGM film are simultaneously finished. Compared to the traditional method, the single-step in-situ preparation method simplifies the manufacturing process and saves time. Furthermore, the size, shape and thickness of KGM film can be easily controlled.

3.3. Ionic conductivity of KGM hydrogel electrolyte

For scrutinizing the ionic diffusion properties after gelating, the ionic conductivity of the KGM hydrogel electrolyte was characterized in the temperature range from 24 °C to 75 °C. As shown in Fig. 5, the dependence of ionic conductivity of the KGM hydrogel electrolyte on the temperature can be described by Vogel–Tammann–Fulcher (VTF) equation:

$$\sigma = AT^{-1/2}\exp\left[-E_a/R(T-T_0)\right]$$

where σ is the ionic conductivity, A is the pre-exponential factor which is related to the concentration of carriers, E_a is the activation energy, R is the molar gas constant, T is the absolute temperature and T_0 is a value relates to ideal glass transition temperature under which the conformational entropy becomes zero and the free volume disappears [38]. T_0 and E_a were obtained from the fitting results. A good fit of the relationship between temperature and ionic conductivity of the KGM hydrogel electrolyte to the VTF equation indicates the influence of polymer chain relaxation on the ion transport. Slightly decreased ionic conductivity at room temperature, from 0.078 to 0.075 S cm^{-1}, is observed after gelating due to the hinder effect of polymer network on ion mobility. However, over 90% of liquid electrolyte in KGM gel can be well trapped into the polymer matrix, leading to no obvious change of the conductivity in order of magnitude after gelating.

3.4. Cell performance of G-QDSCs and L-QDSCs

To investigate the cell performance, we measured the J–V curves of G-QDSCs, L-QDSCs and L-QDSCs without spacer under AM 1.5 as shown in Fig. 6(a). The cell parameters such as the short-circuit current density (J_{SC}), the open-circuit voltage (V_{OC}), the fill factor (FF) and the solar energy to electricity conversion efficiency (η) are shown in Table 1

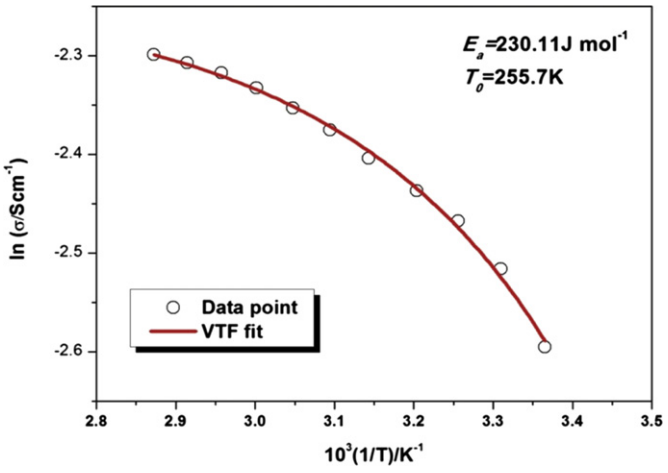

Fig. 5. Temperature-dependent ionic conductivity of KGM hydrogel electrolyte.

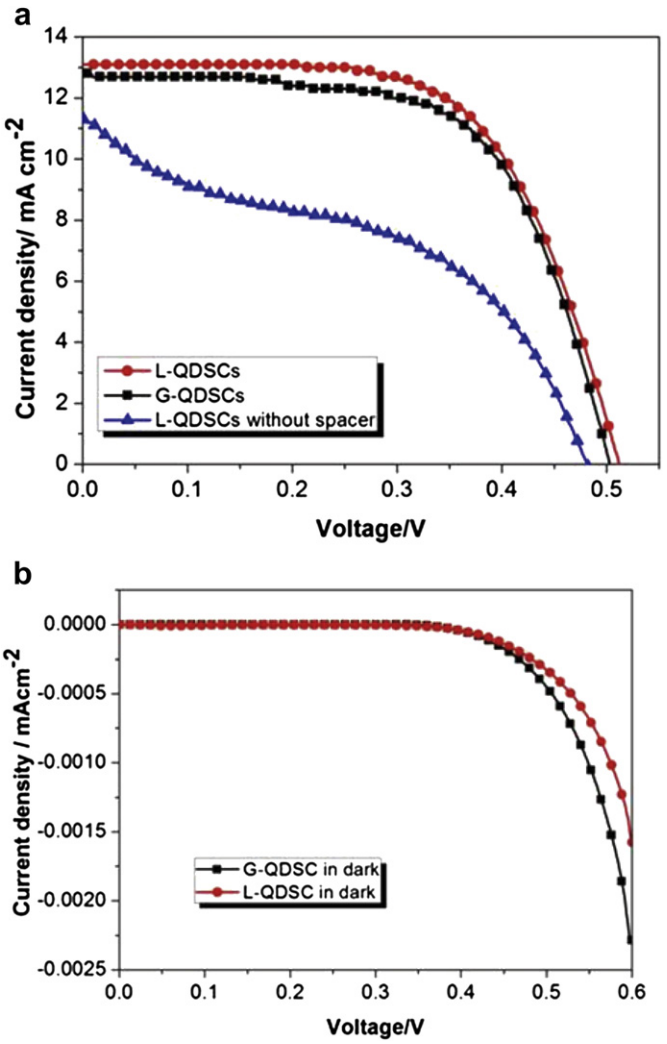

Fig. 6. J–V curves of (a) the G-QDSCs, L-QDSCs and L-QDSCs without spacer under AM 1.5 illumination, (b) the G-QDSCs, L-QDSCs in dark.

As shown in Table 1, the efficiency of L-QDSCs without spacer is only 2.31%. After adding the spacer, the cell performance was significantly improved, indicating that the extremely close contact of TiO_2/QDs and Cu_2S will remarkably increase the recombination reaction and decrease the cell performance as well. Obviously, the existence of the spacer in the fabrication of L-QDSCs is indispensable. In fact, to the G-QDSCs, the thin film gel electrolyte itself can function as both a charge delivery layer and a spacer. The G-QDSCs (4.06%) exhibit very similar cell performance as the L-QDSCs (4.22%). Despite the same fill factor (0.63), both the short-current density and the open-circuit voltage of G-QDSCs are slightly lower than L-QDSCs. Obviously, although the polymer network in G-QDSCs prevents the leakage of polysulfide electrolyte, it restrains the mobility of the diffusion mechanism-controlled redox couple as

Table 1
Cell parameters of QDSCs fabricated with different electrolytes.

	J_{SC} (mA cm^{-2})	V_{OC} (mV)	FF	η (%)
L-QDSCs	13.05	512	0.63	4.22
L-QDSCs (without spacer)	11.41	481	0.42	2.31
G-QDSCs	12.76	503	0.63	4.06

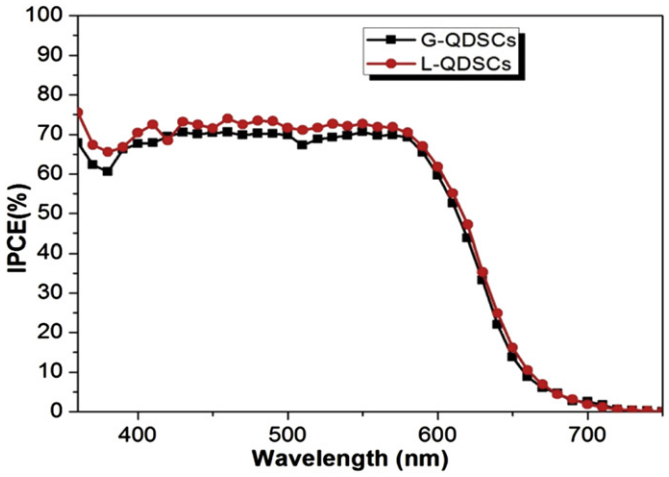

Fig. 7. Comparison between IPCE spectra of G-QDSCs and L-QDSCs.

well. Therefore, in the gel electrolyte, the S_x^{2-} ions, from which the regeneration of oxidized QDs originated, cannot leave the photoanode rapidly as in the liquid electrolyte. It improves the contact possibility between naked TiO_2 and S_x^{2-} after gelating which renders increasing of charge recombination [39]. Fig. 6(b) displays the dark currents of G-QDSC and L-QDSC; the G-QDSC has a slightly higher dark current, indicating a relatively higher charge recombination. Furthermore, we also tried to add an extra spacer in G-QDSC. No change in the cell performance is found to the G-QDSC with and without the spacer. This result indicates that, for the swelling effect of the gel film after adsorbing the liquid electrolyte, the thickness of the gel film is no less than the thickness of the spacer even under the additional pressure of the clips when the gel electrolyte is fabricated in the QDSC.

Fig. 7 shows the incident photon to current conversion efficiencies (IPCE) for G-QDSCs and L-QDSCs at different excitation wavelengths measured from I_{SC} monitored. The IPCE profiles of both cells are almost the same, suggesting the KGM network barely affects the light absorption of QDSCs. In full spectrum range, G-QDSCs have lower IPCE, and their difference is less than 5%.

To further understand the electron transfer and charge recombination at TiO_2/electrolyte interface of L-QDSCs and G-QDSCs, the electrochemical impedance spectroscopy (EIS) for G-QDSCs and

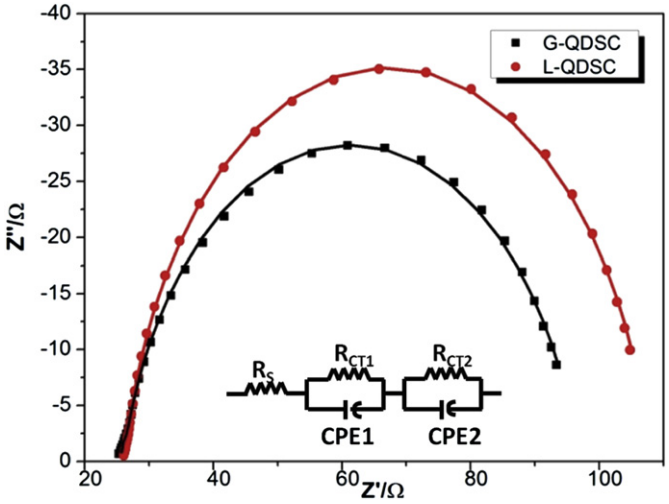

Fig. 8. Electrochemical impedance spectra in Nyquist plots for L-QDSCs and G-QDSCs in dark under forward bias. The inset is the equivalent circuit.

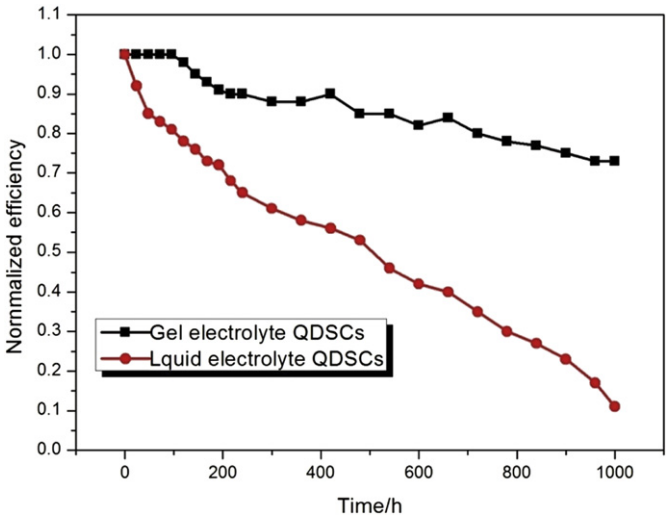

Fig. 9. Time-course change of the normalized efficiency of G-QDSCs and L-QDSCs.

L-QDSCs was carried out under forward bias in dark and the results were analyzed by Z-view using an equivalent circuit containing a constant phase element (CPE) and resistance (R). As shown in Fig. 8, the EIS displays in Nyquist form. As we know, under the circumstance of dark and forward bias, the S^{2-} is oxidized from S_x^{2-} on Cu_2S counter electrode, diffuses through electrolyte to the TiO_2. Then, the electrons which generate from external circuit and inject into the TiO_2 are captured by S_x^{2-}. The last process, essentially corresponding to charge transfer at TiO_2/QD/electrolyte interface, is related to recombination resistance R_{CT2}, the semicircle in middle frequency region in Nyquist diagram [39,40]. According to the fitting results, the sheet resistance (R_s) of G-QDSC is 26.63 Ω and L-QDSC is 26.12 Ω, while the charge transfer resistance (R_{CT1}) of G-QDSCs is 0.248 Ω and L-QDSCs is 0.228 Ω. Hence, no obvious differences are found in R_{CT1}. However, apparent difference in R_{CT2} between G-QDSC and L-QDSC is observed, which are 70.92 Ω and 81.48 Ω, respectively. As we know, R_{CT2} represents the charge transfer in TiO_2/QD/electrolyte interface. The difference of R_{CT2} between L-QDSC and G-QDSC indicate that the back reaction occurring at TiO_2/QD/electrolyte interface enhances due to the introduction of polymer network, which is in agreement with the previous discussion on the dark current and IPCE.

3.5. Stability test of the cells

In order to investigate the stability of KGM hydrogel electrolyte fabricated in QDSCs, both the L-QDSCs and G-QDSCs were sealed. The cells were kept for 1000 h. Under the same sealing and storage condition, G-QDSCs can keep 73% of its original efficiency after 1000 h while the L-QDSCs have dropped to 10%, as shown in Fig. 9. This can be attributed to the strong affinity between polymer matrix and solvent which can prevent the leakage and evaporation of electrolyte [11]. The ability in preventing the leakage and evaporation of solvent results the enhancement of the QDSCs' stability after gelating.

4. Conclusions

In summary, polysaccharide KGM has been firstly applied in quantum dot-sensitized solar cells. The KGM-based gel electrolyte can function as the thin film polymer matrix in QDSCs and the spacer between electrodes as well prepared without mold. Besides, KGM hydrogel electrolyte exhibits the ionic conductivity of

0.074 S cm^{-1} at room temperature, which is quite close to that of liquid electrolyte. A simple single-step in-situ preparation method is developed to produce this gel electrolyte and Cu_2S counter electrode simultaneously. This method can simplify the fabrication process and reduce the manufacturing difficulty. The energy conversion efficiency of G-QDSCs based on KGM gel electrolyte is 4.02%, which has reached up to 96% of the relative L-QDSCs. In the meantime, the stability of QDSCs has been greatly enhanced after introducing KGM quasi-solid state electrolyte.

The single-step in-situ preparation method can be commonly used in QDSCs to fabricate quasi-solid state electrolyte, not just limited to KGM hydrogel. This result will foster widespread practical application of QDSCs. By taking new redox couple into quasi-solid state electrolyte in the future, higher efficiency and more stable QDSCs can be expected.

Acknowledgments

The authors appreciate the financial supports of National Key Basic Research Program (973 project, No. 2012CB932903), National Natural Science Foundation of China (Nos. 20725311, 51072221 and 21173260) and the Knowledge Innovation Program of the Chinese Academy of Sciences (No. KJCX2-YW-W27).

References

[1] B. Oregan, M. Gratzel, Nature 353 (1991) 737–740.
[2] A. Yella, H.W. Lee, H.N. Tsao, C.Y. Yi, A.K. Chandiran, M.K. Nazeeruddin, E.W.G. Diau, C.Y. Yeh, S.M. Zakeeruddin, M. Gratzel, Science 334 (2011) 629–634.
[3] P.V. Kamat, J. Phys. Chem. C 112 (2008) 18737–18753.
[4] W.A. Tisdale, K.J. Williams, B.A. Timp, D.J. Norris, E.S. Aydil, X.Y. Zhu, Science 328 (2010) 1543–1547.
[5] J.B. Sambur, T. Novet, B.A. Parkinson, Science 330 (2010) 63–66.
[6] P.K. Santra, P.V. Kamat, J. Am. Chem. Soc. 134 (2012) 2508–2511.
[7] Q. Zhang, G. Chen, Y. Yang, X. Shen, Y. Zhang, C. Li, R. Yu, Y. Luo, D. Li, Q. Meng, Phys. Chem. Chem. Phys.: PCCP 14 (2012) 6472–6479.
[8] Y.L. Lee, Y.S. Lo, Adv. Funct. Mater. 19 (2009) 604–609.
[9] X.Y. Yu, J.Y. Liao, K.Q. Qiu, D.B. Kuang, C.Y. Su, ACS Nano 5 (2011) 9494–9500.
[10] V. Chakrapani, D. Baker, P.V. Kamat, J. Am. Chem. Soc. 133 (2011) 9607–9615.
[11] P. Wang, S.M. Zakeeruddin, J.E. Moser, M.K. Nazeeruddin, T. Sekiguchi, M. Gratzel, Nat. Mater. 2 (2003) 402–407.
[12] Z. Yu, D. Qin, Y. Zhang, H. Sun, Y. Luo, Q. Meng, D. Li, Energy Environ. Sci. 4 (2011).
[13] D. Qin, Y. Zhang, S. Huang, Y. Luo, D. Li, Q. Meng, Electrochim. Acta 56 (2011) 8680–8687.
[14] Z. Yu, H. Li, K. Li, D. Qin, M. Deng, D. Li, Y. Luo, Q. Meng, L. Chen, Electrochim. Acta 55 (2010) 895–902.
[15] W. Kubo, K. Murakoshi, T. Kitamura, Y. Wada, K. Hanabusa, H. Shirai, S. Yanagida, Chem. Lett (1998) 1241–1242.
[16] W. Kubo, K. Murakoshi, T. Kitamura, S. Yoshida, M. Haruki, K. Hanabusa, H. Shirai, Y. Wada, S. Yanagida, J. Phys. Chem. B 105 (2001) 12809–12815.
[17] W. Kubo, T. Kitamura, K. Hanabusa, Y. Wada, S. Yanagida, Chem. Commun. (2002) 374–375.
[18] P. Wang, S.M. Zakeeruddin, I. Exnar, M. Gratzel, Chem. Commun. (2002) 2972–2973.
[19] M.S. Kang, K.S. Ahn, J.W. Lee, J. Power Sources 180 (2008) 896–901.
[20] F.J. Li, F.Y. Cheng, J.F. Shi, F.S. Cai, M. Liang, J. Chen, J. Power Sources 165 (2007) 911–915.
[21] J.Y. Kim, T.H. Kim, D.Y. Kim, N.G. Park, K.D. Ahn, J. Power Sources 175 (2008) 692–697.
[22] Z. Lan, J.H. Wu, J.M. Lin, M.L. Huang, J. Power Sources 164 (2007) 921–925.
[23] C.L. Chen, H.S. Teng, Y.L. Lee, Adv. Mater. 23 (2011) 4199.
[24] Z. Yu, Q. Zhang, D. Qin, Y. Luo, D. Li, Q. Shen, T. Toyoda, Q. Meng, Electrochem. Commun. 12 (2010) 1776–1779.
[25] Y. Yang, H. Hu, C.-H. Zhou, S. Xu, B. Sebo, X.-Z. Zhao, J. Power Sources 196 (2011) 2410–2415.
[26] W. Wang, X. Guo, Y. Yang, Electrochim. Acta 56 (2011) 7347–7351.
[27] K. Suzuki, M. Yamaguchi, M. Kumagai, N. Tanabe, S. Yanagida, C. R. Chim. 9 (2006) 611–616.
[28] J. Nemoto, M. Sakata, T. Hoshi, H. Ueno, M. Kaneko, J. Electroanal. Chem. 599 (2007) 23–30.
[29] H.-L. Hsu, W.-T. Hsu, J. Leu, Electrochim. Acta 56 (2011) 5904–5909.
[30] M. Alonso-Sande, D. Teijeiro-Osorio, C. Remunan-Lopez, M.J. Alonso, Eur. J. Pharm. Biopharm. 72 (2009) 453–462.
[31] Q. Zhang, X. Guo, X. Huang, S. Huang, D. Li, Y. Luo, Q. Shen, T. Toyoda, Q. Meng, Phys. Chem. Chem. Phys. 13 (2011).
[32] D.M. Li, M.Y. Wang, J.F. Wu, Q.X. Zhang, Y.H. Luo, Z.X. Yu, Q.B. Meng, Z.J. Wu, Langmuir 25 (2009) 4808–4814.
[33] S. Gimenez, I. Mora-Sero, L. Macor, N. Guijarro, T. Lana-Villarreal, R. Gomez, L.J. Diguna, Q. Shen, T. Toyoda, J. Bisquert, Nanotechnology 20 (2009).
[34] X.Z. Guo, Y.H. Luo, Y.D. Zhang, X.C. Huang, D.M. Li, Q.B. Meng, Rev. Sci. Instrum. 81 (2010).
[35] S. Ito, T.N. Murakami, P. Comte, P. Liska, C. Gratzel, M.K. Nazeeruddin, M. Gratzel, Thin Solid Films 516 (2008) 4613–4619.
[36] J.M. De la Fuente, S. Penades, BBA-Gen. Subjects 1760 (2006) 636–651.
[37] M. Maeda, H. Shimahara, N. Sugiyama, Agric. Biol. Chem. Tokyo 44 (1980) 245–252.
[38] I. Albinsson, B.E. Mellander, J.R. Stevens, J. Chem. Phys. 96 (1992) 681–690.
[39] Z. Huo, C. Zhang, X. Fang, M. Cai, S. Dai, K. Wang, J. Power Sources 195 (2010) 4384–4390.
[40] Q. Wang, J.E. Moser, M. Gratzel, J. Phys. Chem. B 109 (2005) 14945–14953.